

3

State of the art in radiation thermometry

3.1. Review of radiation thermometry

Above the freezing point of silver (961,78 °C) the temperature T_{90} [2] is defined by the equation:

$$\frac{L_{\lambda}(T_{90})}{L_{\lambda}[T_{90}(X)]} = \frac{\exp(c_2[\lambda T_{90}(X)]^{-1}) - 1}{\exp(c_2[\lambda T_{90}]^{-1}) - 1} \quad (5)$$

Where $T_{90}(X)$ refers to any one of the silver ($T_{90}(\text{Ag}) = 1234,93$ K), the gold ($T_{90}(\text{Au}) = 1337,33$ K) or the copper ($T_{90}(\text{Cu}) = 1357,77$ K) freezing points and in which $L_{\lambda}(T_{90})$ and $L_{\lambda}(T_{90}(X))$ are the spectral concentrations of the radiance of a blackbody at wavelength λ (in vacuo) at T_{90} and $T_{90}(X)$ respectively, and $c_2 = 0,014388$ m.K.

The only requirements embodied in equation (5) are that the instrument used, a radiation thermometer, be effectively monochromatic and that at least the reference source at temperature $T_{90}(X)$ be a blackbody [7]. A monochromatic radiation thermometer consists of an optical system that includes a wavelength limiting device (such as an interference filter or a colour glass filter) and focuses an image of a source of radiation onto a photodetector. To measure temperatures as prescribed by equation (5), it is necessary to provide some means (e.g. moving the sources or the pyrometer, or altering the optical path) for alternately focusing the two sources onto the detector. The ratio of the two corresponding detector outputs, suitably corrected or interpreted, is then the ratio of the radiances of the two sources at the nominal wavelength of the thermometer.

The optical system of a radiation thermometer is typically constructed from standard, readily obtainable components. Most radiation thermometers use refracting systems, but some, especially if operating beyond the visible region, use reflecting systems.

Radiation thermometry does not demand a large numerical aperture of the optical system; it is typically in the range $f/10$ to $f/20$. Targets, i.e. that part of the source actually viewed by the detector, are nearly always small, as such targets can more readily be arranged to be approximately isothermal and black. (However in the past, and even sometimes today, tungsten strip lamps, although not blackbodies have been used as temperature scale references for radiation thermometry at high temperatures. These were/are calibrated so as to allow for their departure from blackness using the concept of spectral radiance temperature.) Typically a target for a radiation thermometer is circular and about 0,5 mm to 1 mm in diameter. For this reason, and because the radiation thermometer is monochromatic, the only lens aberration of consequence is spherical aberration, and even here the demand is not severe. The lenses (or mirrors) of the radiation thermometer should be corrected for spherical aberration to a level where they become essentially diffraction limited at all apertures at which they will be used. It is convenient if the lenses are achromatic, especially if the radiation thermometer works at a number of wavelengths, particularly if this spans optical and infrared wavelength regions to allow for visual focusing via an auxiliary viewing system. All lenses and mirrors in the system should be of high optical quality and kept absolutely clean to minimize the amount of radiation scattered by imperfections and surface contamination.

A further point to consider in designing an optical system is that of stray radiation from outside the target that can propagate through the system by diffraction, reflection or scattering from the mechanical or optical elements. This effect can have a significant impact on the performance of the radiation thermometer. It is characterised by a quantity known as the “size-of-source effect” [7, 11].

A radiation thermometer can be made effectively monochromatic in many ways, but at present, interference filters are the best choice, due to their high-peak transmittance, narrow bandwidths, high degrees of blocking outside the passband and the fact that they are easily available from many commercial sources. Typical bandwidths are 10 nm, which is a compromise between the smallest detectable temperature difference and the accuracy of the knowledge of the spectral responsivity of the thermometer.

The uncertainty $\Delta T_{90}(\lambda)$ generated by an uncertainty $\Delta\lambda$ in the wavelength is given [7] by

$$\Delta T_{90}(\lambda) = T_{90} \left[\frac{T_{90}}{T_{90}(X)} - 1 \right] \cdot \frac{\Delta\lambda}{\lambda} \quad (6)$$

It is very important that wavelengths outside the passband in regions where the detector is still active be blocked to a level less than one part in 10^4 , of those in the passband. For a filter half width of 10 nm, blocking to a part in 10^5 is required. In addition because the spectral transmittance of an interference filter can vary with its temperature (typically 0,02 – 0,03 nm/°C), the filter temperature should be controlled to about 0,1~0,2 °C .

Actually, most of the radiation thermometers used for the realisation of the ITS-90 use a silicon photodiode as a detector. Typically this type of detector can be used in the wavelength range from 650 nm to values around 900 nm, where they present linearity and stability levels good enough for realising the ITS-90 with low uncertainties [7].

3.2. High temperature eutectic cells

Binary eutectics are formed from two materials that have limited solid solubility in each other [10, 15]. It is possible to see in figure 2 a simplified phase diagram for a mixture of two substances (α and β) that has a eutectic point at E. In this case, α and β have zero solid solubility in each other. The x-axis is the composition (the ratio of α : β in the mix) and the y-axis is temperature. The diagram identifies the phases that are present at a given temperature and composition. Above the liquidus (the solid curves) there is one liquid phase. In section A, there is a mixture of liquid and solid α , in section B a mixture of liquid and solid β . Consider an alloy starting as liquid with a temperature and composition specified by point a. If the system is cooled the coordinates that specify the system will move down until reaching the liquidus at b. At this point solid β will begin to precipitate. Consequently, the liquid will increase in relative amount of α , i.e. the liquid component moves left in the diagram. In fact, as the system cools further and more and more β solid precipitates the composition of

the remaining liquid tracks down the liquidus until it reaches E. At E, the eutectic point, there are three phases present (solid α , solid β and liquid). This is an invariant point; in equilibrium and at constant pressure it defines a unique temperature. Regardless of the starting composition of the alloy there will always be a melt and freeze feature at this eutectic temperature.

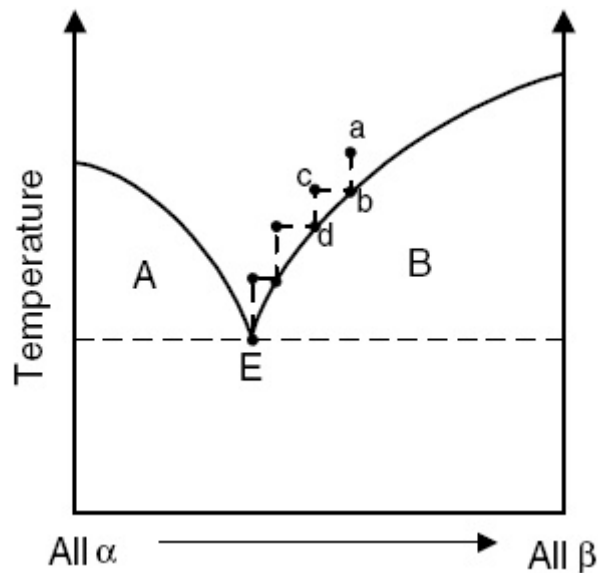


Figure 2: Representation of a typical phase diagram of an alloy that forms a eutectic

The International Temperature Scale of 1990 (ITS-90) presents some alternatives for primary fixed points for radiation thermometry: they are the silver, gold and copper freezing points [2]. Above the temperature of copper, some secondary fixed points have been recommended [16], like the freezing points of nickel (1455 °C) [17], palladium (1554,8 °C) [18] and platinum (1768,2 °C), but none of them have proved to be useful in the long term. The graphite of the crucibles tends to react with metals in a eutectic reaction, depressing the freezing temperature of the metals considerably. Even when other crucible materials were tried, such as alumina, they also proved inadequate, due to the brittleness of alumina crucible [19].

In 1999, Yamada *et al.* [19] proposed the use of high temperature metal-carbon eutectic alloys in graphite crucibles as possible references for thermometry. In this case, as carbon is already a part of the fixed point material, so there is no contamination from the graphite crucible. Possible materials were

selected as candidate high temperature fixed point (HTFP) references that form relatively simple binary phase diagrams.

The first set of metal-carbon eutectic cells were constructed and measured at the National Metrology Institute of Japan, and it was demonstrated that melting temperatures always showed better repeatability than the freezing temperatures, which can be influenced by the cooling rate experienced in the previous freezing. Table 4 shows the melting temperatures of first metal-carbon alloys presented by Yamada *et al* [19]:

Table 4: Melting temperature of some metal-carbon eutectic alloys

Material	Melting temperature (°C)	Reproducibility (°C)
Fe-C	1153	0,13
Ni-C	1329	0,03
Pd-C	1492	0,05
Rh-C	1657	0,08
Pt-C	1738	0,08
Ru-C	1953	0,04

These eutectic cells proved to be robust enough to withstand repeated heat cycles, with the Ni-C cell experiencing 35 cycles, indicating that these fixed points are viable alternatives as practical temperature reference points above the copper point.

Continuing in his studies, Yamada [20 - 22] also proposed four more metal-carbon eutectic cells in 2001. These include the Co-C (1324 °C), the Ir-C (2290 °C), the Re-C (2474 °C) and the Os-C (2732 °C). Only the last one, Os-C, was not used due to formation of an oxide that is hazardous to human health.

Further development in this field included also the realization of metal-carbide-carbon eutectic cells [23], which adds even higher temperature references. These are the TiC-C (2883 °C), the ZrC-C (2927 °C) and HfC-C (3180 °C).

These HTFPs have been the intense study of the high temperature metrology community since their inception and the state of the research is close to the point where they will become more widely accepted as high temperature references [15, 22 - 27].

3.3. Description of the standard pyrometer, the LP3

In metrological laboratories worldwide the radiation thermometer KE LP3 [28] is used for radiation temperature measurements at the highest metrological level and as a transfer standard to establish traceability. With the fundamental principle developed by PTB, the instrument was refined and then commercially manufactured by KE Technologie GmbH, Stuttgart. In essence, it consists of high quality optics with low size-of-source effect [11], well characterised interference filters and a well matched silicon photodiode detector pre-amplifier combination with excellent linear response.

Considering the detector to be linear, it has to generate a photo-current proportional to the incident thermal radiation. For a certain range of sufficient stability of the detectors sensitivity versus incident radiation intensity, as well as versus time, the detector allows the measurement of a radiation intensity ratio in terms of a ratio of photo currents I_1/I_2 . And together with an optical system this is then also valid for radiance ratios L_1/L_2 .

$$\frac{I_1}{I_2} = \frac{L_1}{L_2} \quad (7)$$

Thus, using Planck's equation for the radiance L the unknown temperature of a blackbody can be determined from a radiance comparison with a reference source.

For highest precision measurements only a narrow wavelength interval of the total temperature radiation is selected by an interference filter and one can write for blackbodies at temperatures T_1 and T_2 .

$$\frac{I_1}{I_2} = \frac{L(T_1)}{L(T_2)} = \frac{\exp\left(\frac{c_2}{\lambda_{eff} T_2}\right) - 1}{\exp\left(\frac{c_2}{\lambda_{eff} T_1}\right) - 1} \quad (8)$$

The instrument here is characterised using the concept of the effective wavelength λ_{eff} [11], a single wavelength at which the spectral radiance ratio is equal to the measured radiance ratio for the temperatures T_1 and T_2 . With this method the full integral in the Planck equation does not have to be solved, which

would require an absolute characterisation of the used interference filter, the instruments transmission and the detectors spectral responsivity. Therefore, it follows

$$T_2 = \frac{c_2}{\lambda_{eff}} \left/ \ln \left(\frac{I_1}{I_2} \left(\exp \left(\frac{c_2}{\lambda_{eff} T_1} \right) - 1 \right) + 1 \right) \right. \quad (9)$$

Photo-current I_1 and temperature T_1 can be determined at a blackbody source of known temperature, a reference point or fixed point blackbody. For any measured photo-current I_2 , the temperature T_2 can then be calculated, if λ_{eff} is known.

Using Wien's approximation, Equation (9), λ_{eff} can be calculated directly from the relation

$$\lambda_{eff} = c_2 \left(\frac{1}{T} - \frac{1}{T_{ref}} \right) \left/ \ln \frac{I_{ref}}{I} \right. \quad (10)$$

in an iterative process that usually converges after a few steps.

This measurement principle allows a reliable, low uncertainty realisation of the International Temperature Scale of 1990 (ITS-90) at high temperatures when a gold, silver or copper fixed point blackbody is used as a reference. The LP3 features a silicon detector with advanced electronics to process the photo current signal. The most important design principles of the LP3 are shown in Figure 3 and are described below.

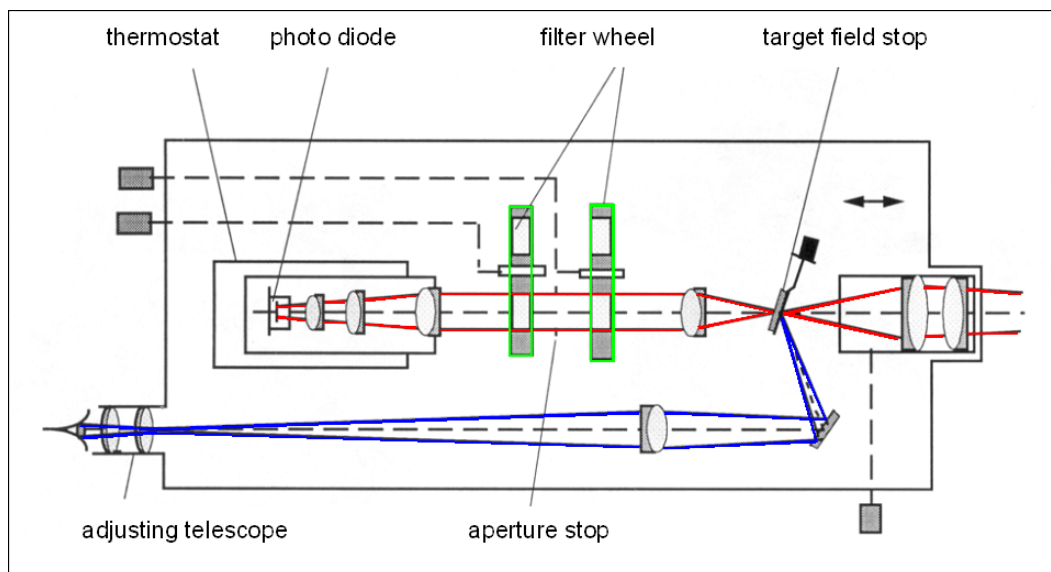


Figure 3: Schematic diagram of the optical design of the LP3

Optical design: The achromatic front lens images the target on the measurement field stop, which consists of a mirror with a 0,2 mm diameter aperture. The reflected light from this mirror passes to an eyepiece, which enables focusing and position alignment. The radiation which passes the aperture in the measurement field stop is collimated onto interference filters, which are mounted in two filter wheels with six filter positions each. Neutral density filters or blocking glasses are preferably mounted in the first filter wheel, while interference filters are mounted in the second filter wheel. The incident radiation is then focused and then detected by a Silicon photodiode positioned in a temperature stabilized housing in the optical path.

Spectral characteristics: Main design features of the interference filters are optimum blocking of the side bands and high long-term stability i.e. preventing ageing through good sealing of the edges of the filter preventing moisture ingress into the filter interference layers due to humid air. Typically a narrow bandwidth of the interference filters of around 10 nm is selected for a low dependency of the effective wavelength on the measured temperature.

The two interference filters of the LP3 S/N 80-42 of the Pyrometry Laboratory of Inmetro, centered at 650 and 900nm were evaluated for spectral transmissivity and at the same time as the spectral responsivity of the radiation detector of the pyrometer, by the Radiometry and Photometry Laboratory of Inmetro, before the beginning of the measurements in this thesis [29]. The results of this evaluation can be seen in figures 4 and 5.

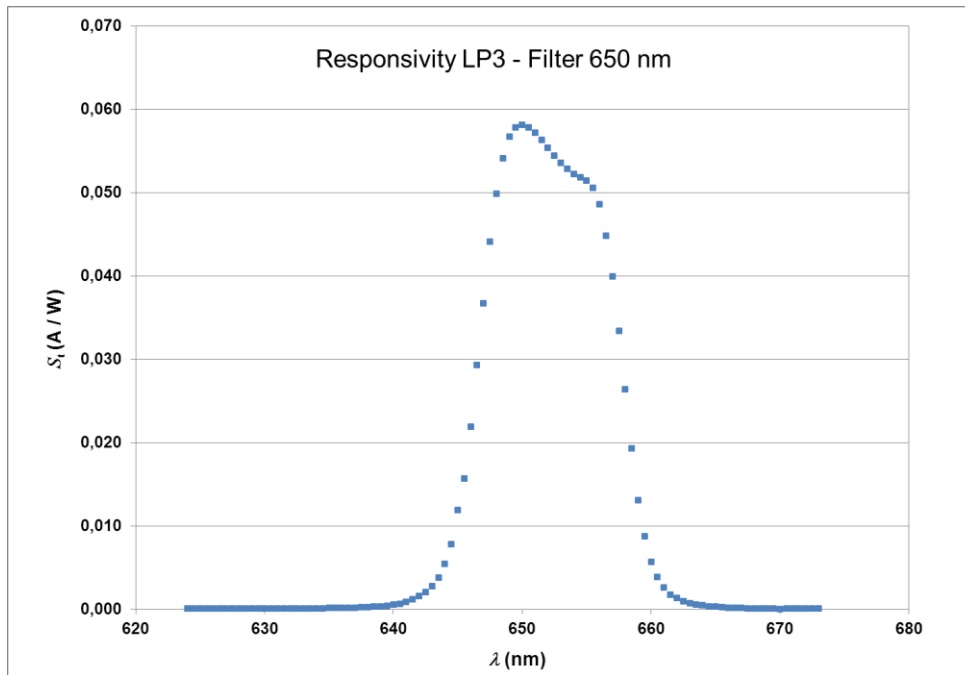


Figure 4: Spectral responsivity curve for 650 nm interference filter

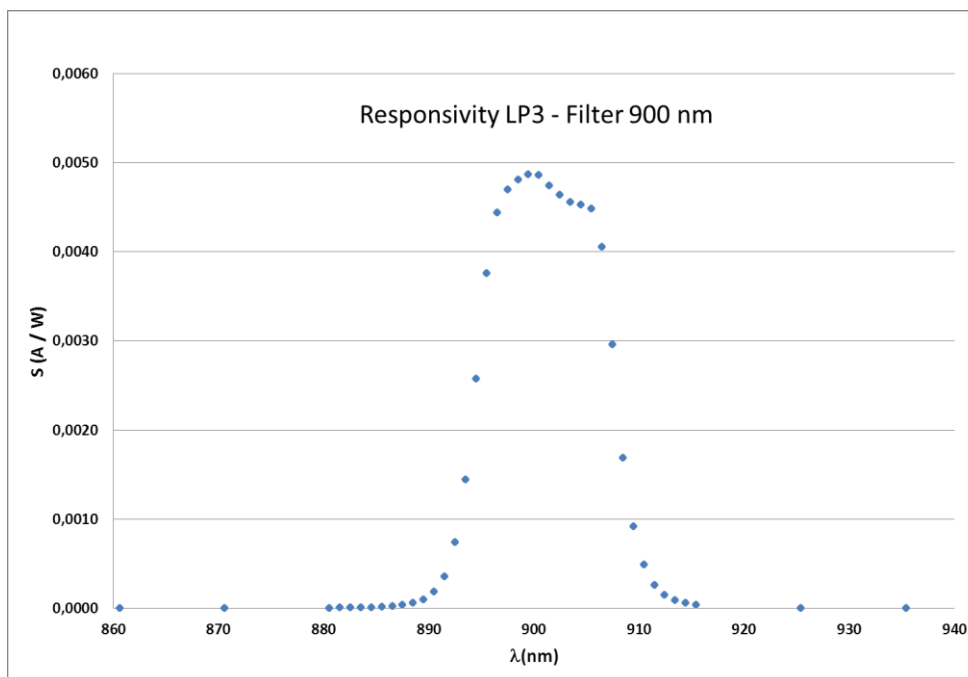


Figure 5: Spectral responsivity curve for 900 nm interference filter

It is worth mentioning that the precision of this data is essential for an accurate determination of the melting point temperature of the HTFP cells developed as part of this research. The veracity of these measurements at Inmetro are justified by the good agreement between the results found at Inmetro and those found at NPL, for the melting point temperature of the Ni-C-Cu#7 and

Ni-C-Cu#8 cells. These details and results of this comparison, the culmination of the work of this thesis, will be presented in detail in chapter 8.